Optical, electrical, and structural properties of amorphous Ag–Ge–S and Ag–Ge–Se films and comparison of photoinduced and thermally induced phenomena of both systems

Takeshi Kawaguchi[a] and Shigeo Maruno
Department of Electrical and Computer Engineering, Nagoya Institute of Technology, Showa-ku, Nagoya 466, Japan

Stephen R. Elliott
Department of Chemistry, University of Cambridge, Lensfield Road, Cambridge CB2 1EW, United Kingdom

(Received 4 December 1995; accepted for publication 15 March 1996)

To understand the nature of Ag-rich chalcogenide glasses, the optical, electrical, and structural properties of evaporated amorphous $(Ge_{0.3}S_{0.7})_{100-x}Ag_x$ and $(Ge_{0.3}Se_{0.7})_{100-y}Ag_y$ films have been examined and compared with each other over a wide compositional range in Ag content. The maximum Ag content for the amorphous films was 67 at. % for the S-based system and 40 at. % for the Se-based system. The physical properties of both systems depended significantly on the Ag content but the compositional trends resembled each other. All the photoinduced and thermally induced phenomena observed for the S-based system were also observed for the Se-based system but with the compositional ranges shifted to lower Ag concentration: the photo- and thermal bleachings ($0 \leqslant y < 22$ for the Se-based system, $0 \leqslant x < 40$ for the S-based system), the photoinduced surface deposition (PSD) of metallic Ag phenomenon, and the phase separation on annealing ($25 < y \leqslant 40$, $50 < x \leqslant 67$). The Se-based system was found to exhibit the PSD phenomenon at low Ag concentrations where the S-based system never exhibits this effect. © *1996 American Institute of Physics.* [S0021-8979(96)07912-1]

I. INTRODUCTION

It is known that Ag-rich Ag–As(Ge)–S glasses exhibit a phenomenon of so-called photoinduced surface deposition (PSD) of metallic Ag, that is, photoinduced segregation of fine Ag particles to the glass surface.[1,2] This effect has attracted interest in application to direct positive patterning with high contrast. However, bulk glasses (maximum Ag content of 45 at. %) have not been suitable samples for this application since the photosensitivity is very much lower than that of conventional photographic films. For the resolving power of Ag pattern printed by PSD, bulk glasses are also inferior to the photographic films, since the photodeposited Ag particles are larger in size than the AgCl(Br) crystallites in the photographic films.

Film samples with much higher Ag contents are necessary to increase the PSD photosensitivity. Therefore, we have studied amorphous Ag-rich Ag–Ge–S films with Ag contents of 60–65 at. %.[3,4] The photosensitivities of these films were 10–100 times greater than those of the bulk glasses but have not yet achieved the level of photographic films. However, with respect to the resolving power of the Ag patterns, these films were comparable or superior to photographic films, since the photodeposited Ag particles were very small in size (less than 0.2 μm in diameter). Further, it was recently found that these films exhibited reversibility in photowriting and thermal erasing of the Ag patterns.[4] This reversibility is an advantage for the application of PSD to new optical recording devices.

To consider the further development for applications, it is essential to know the nature of the Ag-rich chalcogenide films, especially the optical, electrical, and structural properties, since these physical properties are closely related to the mechanism of the PSD phenomenon.[1,5] Furthermore, to understand the physical properties, it is necessary to compare the data obtained for samples with different chalcogenide elements. Therefore, in this study we have prepared Ag-rich Ag–Ge–S films (S-based system) and Ag-rich Ag–Ge–Se films (Se-based system) by co-evaporation of the chalcogenide glasses and metallic Ag. The compositional dependence of the physical properties has been examined for a wide range of Ag contents through measurements of the x-ray diffraction pattern, optical and infrared spectra, dc resistivity, and capacitance.

Differences in the PSD phenomenon between the S- and Se-based systems have also been examined using these samples. The Se-based system was found to exhibit the PSD phenomenon at lower Ag concentrations than the S-based system, suggesting that the Se-based system is superior to the S-based system in regard to the PSD photosensitivity. The relationship between the photoinduced and thermally induced phenomena and the Ag content of the Ag-rich films has been discussed on the basis of data on the optical, electrical, and structural properties for both systems. Several important pieces of knowledge for understanding Ag-rich chalcogenide amorphous films have been obtained in this study.

II. EXPERIMENT

The $(Ge_{0.3}S_{0.7})_{100-x}Ag_x$ system was selected for the S-based system, since the photoinduced and thermally induced phenomena have been previously examined in detail.[6]

[a]Electonic mail: kawa@elcom.nitech.ac.jp

 0021-8979/96/79(12)/9096/9/$10.00

Films in this system ($0 \leqslant x \leqslant 70$) were prepared by co-evaporation of $Ge_{30}S_{70}$ glass fragments and metallic Ag using two W baskets in a vacuum of $\sim 10^{-6}$ Torr. The $(Ge_{0.3}Se_{0.7})_{100-y}Ag_y$ system was selected for study of a Se-based system and the films ($0 \leqslant y \leqslant 50$) were prepared in the same manner as the S-based system using $Ge_{30}Se_{70}$ glass and Ag. The deposition rates of the raw glasses and Ag were separately controlled with two monitor systems to obtain samples compositionally homogeneous throughout the thickness. The respective deposition rates were changed to obtain film samples with various Ag contents: 10–50 Å/s for $Ge_{30}S(Se)_{70}$ glass and 0–50 Å/s for Ag. The deposition time was controlled to adjust the thicknesses of all the films to be 5000 Å. However, there was a scatter of $\pm 4\%$ in the film thicknesses (5000 ± 200 Å). Cleaned quartz glass and Si wafers were used as substrates for the films. The temperature of the substrates was maintained at 20 ± 2 °C by water cooling. The configuration of the substrates and the two monitors was the same as that reported previously.[6]

The Ag content of the film samples was evaluated from the thicknesses of the $Ge_{30}S(Se)_{70}$ and Ag films measured by the respective monitors in the same manner as reported previously.[6] The composition of the samples was checked using an electron-probe microanalyzer (EPMA) (JEOL, JCXA-733) with an energy-dispersive x-ray instrument (Tracor Northern, TN-5500). The raw $Ge_{30}S(Se)_{70}$ glasses and Ag were used as the standard materials for this analysis. It was confirmed that the Ag content estimated using the monitor system was almost equal to that obtained by the EPMA analysis. For the composition of Ge and S(Se), the Ge content of the films was slightly greater than that of the raw $Ge_{30}S(Se)_{70}$ glasses. However, this difference was within the experimental error of the EPMA analysis.

The experimental procedures for x-ray diffraction, scanning electron microscopy (SEM), optical and infrared spectroscopy, and for measurements of dc resistivity and capacitance have been described in our recent article.[7]

The photoinduced and thermally induced phenomena of the films were examined after the films were placed in an optical cryostat kept in a vacuum of $\sim 10^{-3}$ Torr. Illumination was provided with light from a 500 W Xe lamp (Ushio–Denki) through an ir-cut filter. Annealing was done at a temperature of 150 °C. All the experiments on the as-deposited films were carried out immediately after the film preparations, because thermal bleaching of the films proceeds at an appreciably high rate even at room temperature.[6]

III. RESULTS

The open and closed circles in Fig. 1 show the compositions of the S-based and Se-based films, respectively, prepared in this study. The Ag contents were $x=0$, 20, 28, 38, 52, 60, 67, and 70 at. % for the S-based system and $y=0$, 18, 22, 30, 35, 40, and 50 at. % for the Se-based system. The surface of all the as-deposited films, except for the compositions $x=70$ and $y=50$, was mirrorlike and the color ranged from white–yellow to black for the S-based system, and from orange–yellow to black for the Se-based system, with an increase in Ag content. The surface of the films with $x=70$ and $y=50$ was lusterless and brilliant white in color.

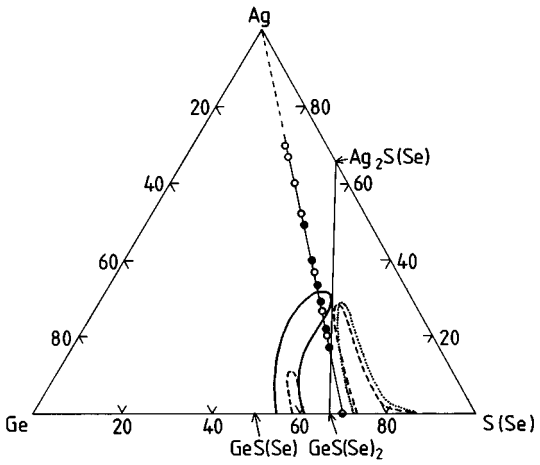

FIG. 1. Phase diagram of the Ag–Ge–S(Se) system and compositions of the film samples prepared in this study. The open circles on the tie line between $Ge_{30}S_{70}$ and Ag show the compositions in the $(Ge_{0.3}S_{0.7})_{100-x}Ag_x$ system: $x=0$, 20, 28, 38, 52, 60, 67, and 70. The closed circles on the tie line between $Ge_{30}Se_{70}$ and Ag show the compositions in the $(Ge_{0.3}Se_{0.7})_{100-y}Ag_y$ system: $y=0$, 18, 22, 30, 35, 40, and 50. The solid and dashed curves show the homogeneous glass-forming regions of the Ag–Ge–S[8] and Ag–Ge–Se[9] systems, respectively. The dotted curve on the S-rich side of the GeS_2–Ag_2S tie line shows another homogeneous glass-forming region of the Ag–Ge–S system found in this study.

The homogeneous glass-forming regions of the Ag–Ge–S(Se) system are also shown in Fig. 1. The solid curve shows the region of the Ag–Ge–S system reported by Kawamoto and Tsuchihashi[8] and it is located only at the Ge-rich side of the GeS_2–Ag_2S tie line. The dashed curves show the glass-forming regions of the Ag–Ge–Se system reported by Borisova *et al.*[9] and they are located on either side of the $GeSe_2$–Ag_2Se tie line. This difference, one region for the Ag–Ge–S system and two regions for the Ag–Ge–Se system, seems to be strange. Therefore, in the early stage of this study, we checked the glass-forming region of the Ag–Ge–S system under almost the same conditions as reported by Kawamoto and Tsuchihashi.[8] We obtained the same glass-forming region as reported by them on the Ge-rich side of the GeS_2–Ag_2S tie line. However, it was found that there was another homogeneous glass-forming region on the S-rich side, as shown by the dotted curve in Fig. 1. The shape, size, and location of this region are very similar to those characteristic of the glass-forming region on the Se-rich side for the Ag–Ge–Se system.

A. X-ray diffraction patterns

Figure 2 shows x-ray diffraction patterns of the as-deposited films for the S-based system. The patterns for samples with up to 60 at. % Ag do not show any crystalline peaks and the peaks for Ag metal are only seen in the pattern for $x=70$. This result suggests that the films with $0 \leqslant x \leqslant 60$ are amorphous. It seemed by SEM observation that these amorphous films were homogeneous [see (a) in Fig. 10]. On the other hand, a large number of white spots were observed by SEM for the film surface of $x=70$. These spots were confirmed to be fine particles of pure Ag by EPMA analysis. This result suggests that the appearance of a white and lus-

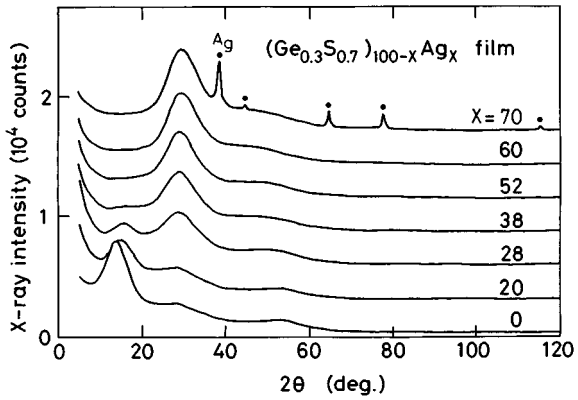

FIG. 2. X-ray diffraction patterns of as-deposited $(Ge_{0.3}S_{0.7})_{100-x}Ag_x$ films (S-based system). The peaks marked by the small closed circles on the $x=70$ pattern correspond to peaks of metallic crystalline Ag.

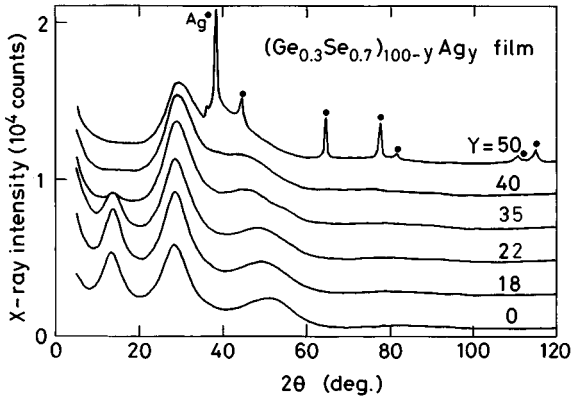

FIG. 3. X-ray diffraction patterns of as-deposited $(Ge_{0.3}Se_{0.7})_{100-y}Ag_y$ films (Se-based system). The peaks marked by the small closed circles on the $y=50$ pattern correspond to peaks of metallic crystalline Ag.

terless film surface for this composition is due to the fine Ag particles deposited on the surface during preparation.

A film with $x=67$ was also prepared, although the x-ray pattern is not shown in Fig. 2. This film was partially inhomogeneous on a macroscopic scale, since sparse small, white, and lusterless domains were observed on a smooth black surface by using an optical microscope. A sample of this composition with a large smooth surface unfortunately could not be obtained in this study. Therefore, the x-ray diffraction pattern and infrared transmission spectrum could not be taken for this sample, because these experiments need samples with a large size over 2.5×2.5 cm^2 to obtain reliable data. However, data on optical and electrical properties could be obtained, since samples with a small size (1×0.5 cm^2) were sufficient for the experiments.

Although the film with $x=67$ was partially inhomogeneous on a macroscopic scale, we regard the maximum Ag content of amorphous films for the S-based system as 67 at. %, since this value agrees with the maximum Ag content reported previously (66 at. %,[3] 67 at. %).[4] It seems that $Ge_{30}S_{70}$ films cannot contain more than 67 at. % Ag and that the excess Ag deposits as elemental metal on the film surface during preparation.

Figure 3 shows x-ray diffraction patterns of the as-deposited films for the Se-based system. The patterns for samples up to 40 at. % do not show any crystalline peaks and the peaks for Ag metal are only seen in the pattern for $y=50$. The film with $y=40$ was slightly inhomogeneous on a macroscopic scale. However, since samples with a large smooth surface could be obtained, in contrast to the films with $x=67$ for the S-based system, all the experiments could be carried out using these samples. We regard the maximum Ag content of amorphous films for the Se-based system to be 40 at. % in the same way as for the S-based system. For the film with $y=50$, it is also suggested that a large number of fine particles of pure Ag were deposited on the surface during preparation.

In Fig. 2 for the S-based system, the first diffraction halo at around $2\theta=15°$ (Cu $K\alpha$), the first sharp diffraction peak (FSDP), shifts toward higher angles with increasing Ag content. The intensity decreases with an increase in the Ag concentration and becomes negligible at $x=38$. The second halo at around $2\theta=30°$ also shifts toward higher angles but the intensity increases with an increase in Ag content. The same features can be observed for the Se-based system but there the FSDP becomes negligible at $y=35$, as shown in Fig. 3.

B. Infrared and optical transmission spectra

Figure 4 shows the infrared transmission spectra of as-deposited films for the S-based system. The spectrum with $x=0$ ($Ge_{30}S_{70}$) is almost the same as the spectrum for an as-deposited $Ge_{27}S_{73}$ film reported by Tichy *et al.*[10] The ab-

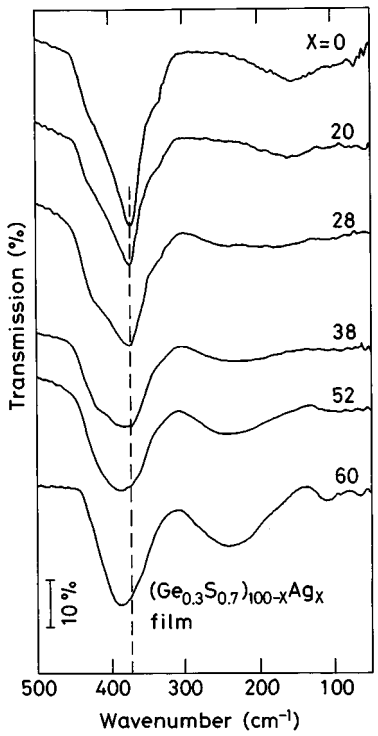

FIG. 4. Infrared transmission spectra of as-deposited films for the S-based system. The dashed line at around 370 cm^{-1} indicates the position of the fundamental Ge–S vibration band.

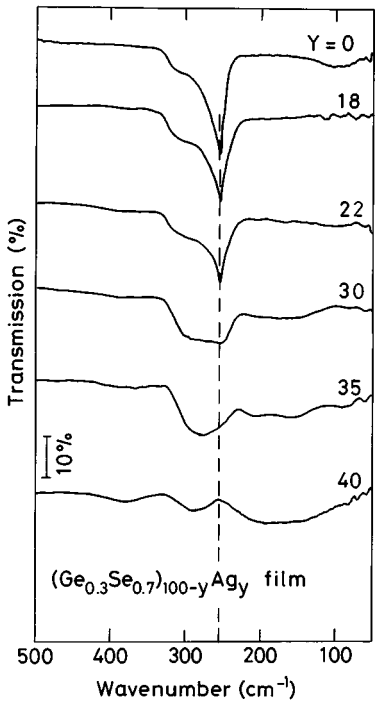

FIG. 5. Infrared transmission spectra of as-deposited films for the Se-based system. The dashed line at around 250 cm^{-1} indicates the position of the fundamental Ge–Se vibration band.

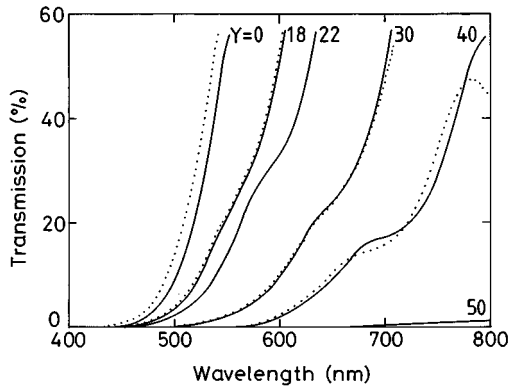

FIG. 6. Optical transmission spectra of as-deposited films for the Se-based system and for the illuminated films. The solid curves show the spectra of the as-deposited films and the dotted curves show the spectra after exposure to light from a Xe lamp (110 mW/cm^2) for 30 min at 20 °C.

sorption band of the fundamental Ge–S vibration at 370 cm^{-1} broadens and its intensity decreases with an increase in the Ag content. For films with $x \geqslant 38$, another broad peak appears in the region of 200–300 cm^{-1} and the peak is dominant in the spectrum for the film with $x=60$. From this result, it is suggested that Ag atoms incorporated in $Ge_{30}S_{70}$ films break up the Ge–S network structure through the formation of Ag–S bonds. The Ag–S bonds become dominant in the Ag-rich films with $x \geqslant 38$ and the breakup of the Ge–S network structure is associated with the disappearance of the FSDP in the x-ray patterns.

Figure 5 shows the infrared transmission spectra of the as-deposited films for the Se-based system. The spectrum with $y=0$ ($Ge_{30}Se_{70}$) is almost the same as the spectrum for an as-deposited $Ge_{31}Se_{69}$ film reported by Tichy *et al.*[11] The absorption band of the fundamental Ge–Se vibration at 250 cm^{-1} broadens and its intensity decreases with increasing Ag content. For films with $y \geqslant 30$, another broad peak appears in the region of 100–200 cm^{-1} and this peak is dominant in the spectrum for the film with $y=40$. The changes in the spectra between $y=22$ and 30 seem to be more remarkable in comparison with the changes between $x=28$ and 38 for the S-based system.

Figure 6 shows the optical transmission spectra of the as-deposited films for the Se-based system. The data for the S-based system have been given in Refs. 3 and 6. In Fig. 6, the spectra shift to longer wavelength with an increase in Ag content. This result agrees with the change in color of the films observed by eye (from orange–yellow to black). The very low transmission of the film with $y=50$ is due to the scattering associated with the lusterless surface. Furthermore, the brilliant white color can be explained by reflection and scattering of light from the fine Ag particles on the film surface.

Figure 6 also shows the spectra after illumination (dotted curves). Changes in the spectra on illumination are observed for all the films except for that with $y=22$. The blueshifts exhibited by films with $y=0$ and 18 are due to the photobleaching phenomenon[6,7] and seem to decrease with an increase in Ag content. The changes exhibited by films with $y=30$ and 40 are due to the PSD phenomenon[4,6] and seem to increase with increasing Ag content.

A blueshift was also observed for annealed films with $y=0$ and 18. This shift is due to the thermal bleaching phenomenon[6,7] and decreased with increasing Ag content with the same tendency as for photobleaching. The films with $y=30$ and 40 exhibited a spectral change on annealing. This change is due to phase separation into Ag-poor and Ag-rich phases, as observed for the S-based system.[6] The phase separation was confirmed by SEM observation. Furthermore, the Ag concentrations of the respective phases were evaluated by EPMA analysis to be ~22 at. % for the Ag-poor phase and ~45 at. % for the Ag-rich phase. The relationship between these spectral changes on annealing and the Ag content is discussed later when comparing with the data for the S-based system.

The optical transmission edge (λ_{edge}) of the as-deposited films for S- and Se-based systems was evaluated as a function of Ag content, as shown in the right ordinate in Fig. 7. We defined λ_{edge} as the wavelength corresponding to 5% transmission in the same way as reported previously.[7] In this study, since the film thicknesses were 5000 Å, the value of λ_{edge} on a scale of photon energy (eV) corresponds to an optical band gap with an optical absorption coefficient (α) of 6×10^4 cm^{-1}.[7] Since the value of λ_{edge} depends on the film thickness, the scatter of values of film thickness studied was kept within ±4% (5000±200 Å), as mentioned in Sec. II.

The photon energy thus determined at $\alpha=6\times10^4$ cm^{-1} for the as-deposited $Ge_{30}S_{70}$ film (3.4 eV) is consistent with the photon energy reported by Tichy *et al.*[12] (3.5 eV at the same α for an as-deposited $Ge_{30}S_{70}$ film). Furthermore, the

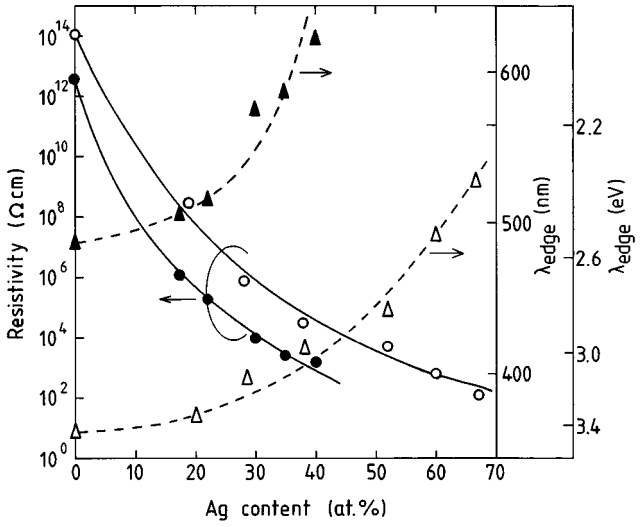

FIG. 7. DC resistivity (ρ_{dc}) and optical transmission edge (λ_{edge}) of as-deposited films for S- and Se-based systems as a function of Ag content. The open and closed circles show ρ_{dc} of the S- and Se-based films, respectively. The open and closed triangles show λ_{edge} of the S- and Se-based films, respectively. The quantity λ_{edge} is evaluated as the wavelength corresponding to 5% transmission.[7] All the data were obtained at 20 °C.

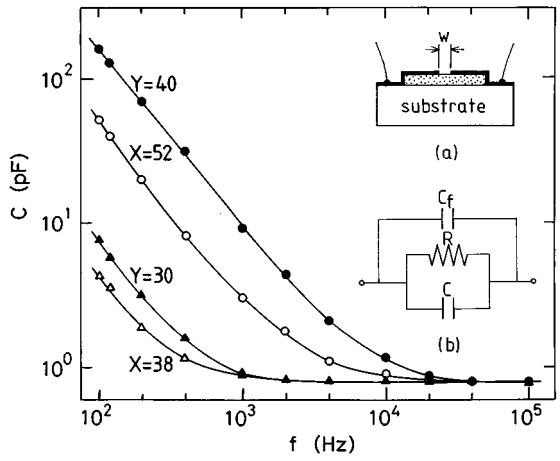

FIG. 8. Frequency dependence of the capacitance of as-deposited films for S- and Se-based systems. The open circles and triangles show the raw data for S-based films ($x=52$ and 38) and the closed circles and triangles show the raw data for Se-based films ($y=40$ and 30). All the data were obtained at 20 °C. The inset (a) shows the sample used in this experiment with planar gap-cell geometry for the electrode configuration ($w=180$ μm). The inset (b) shows the equivalent circuit of the sample, where C and R are the capacitance and resistance of the films, respectively. C_f represents the floating capacitance of the sample.

photon energy for the as-deposited $Ge_{30}Se_{70}$ film (2.5 eV) is consistent with that of an as-deposited $Ge_{33}Se_{67}$ film (2.4 eV at the same α) reported by Theye *et al.*[13] As shown in Fig. 7, the optical band gap corresponding to $\alpha=6\times10^4$ cm^{-1} decreases with an increase in Ag content for both systems and the compositional trends resemble each other.

C. Resistivity and capacitance

Two types of samples were prepared with different electrode configurations for measurement of the dc resistivity (ρ_{dc}). The sandwich type was used for $0\leqslant x\leqslant 20$ for the S-based system and $0\leqslant y\leqslant 18$ for the Se-based system, since these films have high resistivities. The planar gap-cell type [see the inset (a) in Fig. 8] was used for the other low-resistivity films. For the sandwich type, we prepared films with thicknesses greater than 5 μm to avoid short circuits between the sandwich electrodes through pinholes in the films. Values of ρ_{dc} of the films with low Ag concentration ($0\leqslant x\leqslant 20, 0\leqslant y\leqslant 18$) were measured using a dc field. On the other hand, values of ρ_{dc} of the Ag-rich films ($x\geqslant 28, y\geqslant 22$) were evaluated from the frequency dependence of the ac resistivities from 100 to 5000 Hz (Cole–Cole plots),[5] extrapolated to zero frequency, since these films exhibit a marked ionic conduction of Ag^+ ions under a dc field.

Figure 7 also shows ρ_{dc} of the as-deposited films for S- and Se-based systems as a function of Ag content. The value of ρ_{dc} of the $Ge_{30}S_{70}$ film (10^{14} Ω cm at 20 °C) is close to ρ_{dc} of bulk glassy GeS_2 reported by Nagels *et al.*[14] (10^{14} Ω cm at 60 °C). The value of ρ_{dc} of the $Ge_{30}Se_{70}$ film (5×10^{12} Ω cm at 20 °C) is between that of the two bulk glasses $Ge_{22}Se_{78}$ (Ref. 15) [10^{12} Ω cm at 20 °C] and $GeSe_2$ (Ref. 16) [10^{14} Ω cm at 20 °C by extrapolation of ρ_{dc} data for 80–350 °C]. Furthermore, ρ_{dc} of the film with $x=28$ ($Ag_{28}Ge_{22}S_{50}$) has the same order of magnitude as $Ag_{28}Ge_{20}S_{52}$ bulk glass[17] ($\sim10^5$ Ω cm at 20 °C). As shown in Fig. 7, ρ_{dc} for both systems drastically decreases with increasing Ag content. The value of ρ_{dc} for the S-based films is about 100 times greater than ρ_{dc} for the Se-based films with the same Ag content over the range $20\leqslant(x,y)\leqslant 40$, but the compositional trends of both systems strongly resemble each other.

The electrical conduction of the Ag-rich films is governed by ionic conduction of Ag^+ ions (superionic conductor). The dc conductivity σ_{dc} is given by $\sigma_{dc}=1/\rho_{dc}=ne\mu$, where n and μ are the concentration of the movable Ag^+ ions and their mobility, respectively. Therefore, the 100 times difference in ρ_{dc} is attributable to n and/or μ, since e is a constant. Miyamoto *et al.*[18] recently suggested, from data obtained using a time-of-flight method, that n of Ag-rich Ag–As–S bulk glasses (15–45 at. % Ag) is constant ($\sim10^{19}$ cm^{-3}) and μ increases exponentially with increasing Ag content. That is, according to their suggestion, the conductivity of the Ag-rich glasses depends only on μ. Therefore, to obtain information about the movable Ag^+ ions in the Ag-rich S- and Se-based films, we have examined the frequency dependence of the capacitance.

Figure 8 shows the raw capacitance data from 10^2 to 10^5 Hz. The capacitance of the Ag-rich films is very large at low frequencies and markedly decreases with an increase in frequency. On the other hand, the capacitance of $Ge_{30}S(Se)_{70}$ films was very low ($\sim$0.9 pF) and a frequency dependence was not observed. Therefore, the frequency dependence of the Ag-rich films is due to the ionic conduction of Ag^+ ions and the high capacitance at low frequencies can be explained by the formation of a thin depletion layer of Ag^+ ions near the positive Au electrode.[19]

The insets in Fig. 8 show the sample (planar gap-cell type) used in this capacitance experiment and the equivalent

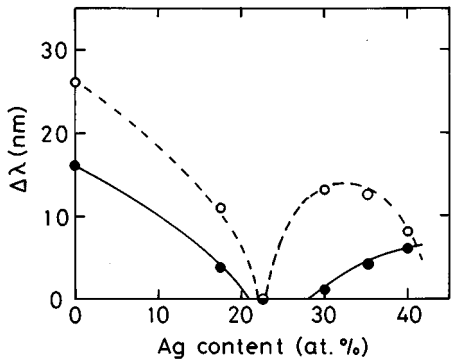

FIG. 9. Composition dependence of Δλ for the Se-based system, where Δλ denotes the wavelength shift of the optical transmission spectrum on illumination or annealing. The value of Δλ was evaluated as the change in wavelength corresponding to 15% transmission.[6] The closed circles show Δλ after illumination (Xe lamp, 110 mW/cm^2, 30 min, 20 °C). The open circles show Δλ after annealing (150 °C, 1.5 h, in Ar gas). A positive value of Δλ means a shift to shorter wavelength (blueshift):[6] $\Delta\lambda=\lambda_{T=15\%}$ (as-deposited film)$-\lambda_{T=15\%}$ (illuminated or annealed film), where $\lambda_{T=15\%}$ is the wavelength corresponding to 15% transmission.

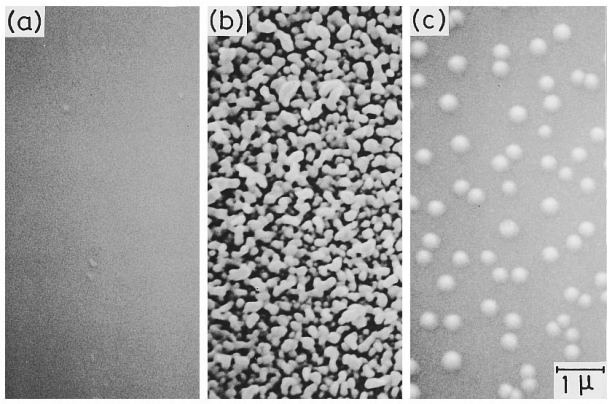

FIG. 10. Electron scanning microphotographs of surfaces of Ag-rich films for S- and Se-based systems: (a) an as-deposited film with $x=60$ (S-based system), (b) an illuminated film with $x=60$, (c) an illuminated film with $y=35$ (Se-based system). The surface of the as-deposited film with $y=35$ was as smooth as (a). Illumination was provided with light from a Xe lamp (110 mW/cm^2) through an ir-cut filter at 20 °C for (b) 5 min and (c) 30 min. All the photographs are to the same scale.

circuit. The sandwich type is usually preferable for capacitance measurements, since the floating capacitance can be neglected for the film samples. However, thick films with high Ag concentrations could not be obtained in this study because of the low heating power of the evaporation system. The capacitance of all the samples is observed to approach a constant level of ~0.9 pF at high frequency, since the sample capacitance (C) becomes less than the floating capacitance (C_f) in this frequency region.

In Fig. 8, the capacitance at low frequency (for example, 100 Hz) increases with increasing Ag content for both systems and the capacitance of the Se-based system is greater than that of the S-based system with the same Ag content. On the other hand, the capacitance of all the samples decreases in an almost parallel fashion from low to high frequencies. Therefore, samples with higher Ag content exhibit a capacitance greater than the C_f level up to higher frequencies. If Ag^+ ions can move fast and can follow the alternating electric field with high frequency, a large capacitance due to the Ag^+ movement seems to be observable up to the higher frequency region. However, further interpretation is difficult at the present stage because of a lack of detailed information about the thin depletion layer of Ag^+ ions.

IV. DISCUSSION

A. Photoinduced and thermally induced phenomena

Figure 9 shows the shift in the optical transmission spectra induced by illumination and annealing as a function of Ag content. These are data for the Se-based system; the data for the S-based system are given in Ref. 6. The magnitude of the shift was evaluated by the change in wavelength at 15% transmission (Δλ) in the same way as reported previously.[6] The values of Δλ were almost the same as those evaluated at 5% transmission, since the spectra shift in a parallel fashion (see Fig. 6 in this article and Fig. 10 in Ref. 6). A positive value of Δλ means a shift to shorter wavelength (blueshift):[6] $\Delta\lambda=\lambda_{T=15\%}$ (as-deposited film)$-\lambda_{T=15\%}$ (illuminated or annealed film), where $\lambda_{T=15\%}$ is the wavelength corresponding to 15% transmission.

For the range $0\leqslant y<22$ (Δλ decreases with an increase in Ag content), the shifts induced by illumination and annealing are considered to be due to photobleaching and thermal bleaching phenomena, respectively, since the compositional trends are similar to those of the S-based system ($0\leqslant x<40$).[6] Therefore, in the same way as for the S-based system, the compositional trends can be accounted for by supposing that Ag atoms incorporated in the Se-based films break up the Ge–Se network structure through the formation of Ag–Se ionic bonds. The photobleaching observed for low values of x, y is namely possible photoinduced bond breaking and subsequent rebonding (polymerization) processes, as for as-deposited chalcogenide films.[6]

In the range $22<y\leqslant 40$, the shifts induced by illumination and annealing are considered to be due to the PSD phenomenon and phase separation, respectively. Similar compositional trends have also been observed for the S-based system ($45<x\leqslant 67$).[6]

Figure 10 shows a comparison using SEM of PSD phenomena for both S- and Se-based systems. In (b), more Ag particles are deposited in a shorter illumination time in comparison with (c). Therefore, at first sight, the Se-based films seem to exhibit a low sensitivity for the PSD phenomenon. However, these samples are very different with respect to the Ag content ($x=60$, $y=35$) and the S-based films with the low Ag content of 35 at. % never exhibit the PSD phenomenon. Therefore, if Se-based samples with the high Ag content of 60 at. % could be obtained as amorphous films, it is expected that the Se-based film would be more sensitive for the PSD phenomenon than the S-based film with $x=60$.

The PSD phenomenon has been observed in Ag-rich Ag–As(Ge)–S glasses or films and the related Ag-rich crystalline compounds did not exhibit PSD.[1,4] Therefore, we have considered that the PSD phenomenon is limited to thermodynamically unstable glasses containing a large amount

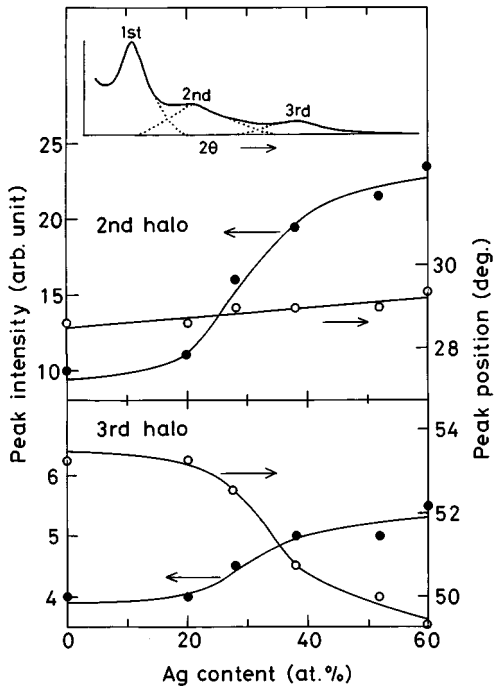

FIG. 11. Peak intensity and position of 2nd and 3rd haloes in x-ray diffraction patterns as a function of Ag content. The data are for as-deposited films for the S-based system. The closed and open circles show the peak intensity and position of the haloes, respectively. The inset illustrates the decomposition of the respective haloes in the x-ray patterns.

of Ag and is a photochemical reaction toward a thermodynamically stable state with segregation of excess Ag atoms in the glass.[1] Further, to explain the movement of Ag in the PSD process, we have considered that a photoelectronic-ionic interaction is necessary for the Ag migration toward the illuminated surface.[5] This means that Ag^+ ions in the glasses can move fast. In this connection, we recently found that Cu-rich Cu–Ge–S films did not exhibit the PSD phenomenon (even with a Cu content of 62 at. %) because of the absence of ionic conduction of Cu in the films.[7]

Therefore, the PSD photosensitivity is suggested to depend on both the thermodynamical instability of the Ag-rich glasses and the diffusivity of Ag^+ ions in the glasses. These factors are closely connected to each other and seem to become greatest at around the maximum Ag content. In fact, for all the systems which have been yet examined, the appearance of the PSD phenomenon is limited to near the maximum Ag content.

B. Structure of Ag-rich films

As demonstrated by the x-ray patterns and infrared spectra, the structure of S- and Se-based films depends significantly on the Ag content. A marked change seems to appear between $x=20$ and 38 for the S-based system and between $y=18$ and 30 for the Se-based system. Correspondingly, different photoinduced and thermally induced phenomena are observed: photo- and thermal bleaching at low Ag concentrations and the PSD phenomenon and phase separation at high Ag content.

Figure 11 shows the peak intensity and position of the 2nd and 3rd haloes in the x-ray diffraction patterns of Fig. 2 (S-based system). A marked change in observed between 20 and 40 at. % Ag, except for the peak position of the 2nd halo. In addition to the change in these haloes, the FSDP is observed to disappear at around 40 at. % Ag (see Fig. 2). A similar tendency is observed for the Se-based system. However, the marked change appears at a lower composition range (between 15 and 30 at. %) and the FSDP disappears at around 30 at. % Ag.

A similar decrease in intensity of the FSDP with addition of a network modifier has also been observed in the cases of the corresponding bulk glasses, namely studies by neutron diffraction of a glass in the Ag–Ge–Se system[20] and of three compositions in the $(Ag_2S)_x(GeS_2)_{1-x}$ system[21] ($x=0.3$, 0.4, and 0.5). Furthermore, the intensity of the second peak in the neutron-derived distinct scattering function for the $(Ag_2S)_x(GeS_2)_{1-x}$ glass system was also observed[21] to increase approximately linearly with increasing Ag content, x, i.e., very similar to the behavior found in this study (Fig. 11). Thus, amorphous films and bulk glasses appear to behave in a similar structural way in this regard. This compositional behavior, a decrease in the FSDP intensity and an increase in the second-peak intensity with increasing Ag modifier content, has been explained[21] in terms of the void model[22] for the origin of the FSDP. In this model, interstitial voids that are chemically ordered around cation-centered structural units [e.g., $GeS(Se)_4$ tetrahedra] are responsible for the production of the FSDP as a chemical-order prepeak. Extrinsic atoms (e.g., Ag) then are assumed to occupy these interstitial voids, thereby reducing the neutron-scattering contrast and hence the intensity of the FSDP. The increase in intensity of the second peak in the diffraction pattern with increasing Ag content is merely a consequence of the change in average neutron scattering length (or x-ray scattering factor) with Ag content.[21]

Such changes are also observed for the infrared spectra of both systems. It was found that the spectra could be decomposed into two absorption components corresponding to Ag-poor and Ag-rich phases. Figure 12 shows the procedure of the decomposition. For simplicity, it is assumed that the spectrum of the Ag-poor phase is the same as that of the film with $y=22$. The dotted curves in (a) show the absorption component of the Ag-poor phase matched by a suitable scaling. The residue after subtraction of the component is considered to be the absorption component of the Ag-rich phase. As shown in (b), the residues for the films with $y=30$ and 35 are similar to each other and resemble the spectrum of $y=40$ (see Fig. 5). Therefore, phase separation of the as-deposited Se-based films is suggested to occur above 30 at. % Ag, although clear evidence could not be obtained by SEM observation. Such decomposition was also available for the S-based system and the phase separation seemed to occur above 38 at. % Ag.

The idea of phase separation on a microscopic scale can be supported by the data of the annealed films. As mentioned in Sec. III B, the Ag-rich films of both systems exhibited phase separation into Ag-poor and Ag-rich phases on annealing at 150 °C for 1.5 h and the phase separation was confirmed by the change in the optical transmission spectra and by SEM observation. It seems that the diffuse boundary be-

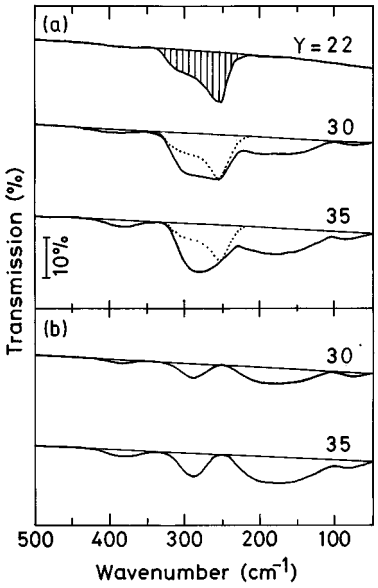

FIG. 12. Decomposition of absorption components in infrared spectra of as-deposited films for the Se-based system. The upper figure (a) shows the subtraction of the absorption component of $y=22$ (hatched area) from the spectra of $y=30$ and 35 (solid curves). The dotted curves are the absorption components matched by a suitable scaling. The lower figure (b) shows the residual components after the subtraction.

tween Ag-poor and Ag-rich phases for the as-deposited films was made clear by the annealing.

Figure 13 shows a schematic illustration of the phase separation model. (a) shows the films with low Ag concentration ($x<45$, $y<22$). the small dots schematically represent the Ag concentration and do not signify phase separation. (b) shows the films completely comprising the Ag-poor phase ($x=\sim45$, $y=\sim22$). The photo- and thermal bleaching become negligible and the FSDP disappears at this stage. (c) shows the phase-separated films ($x=\sim50$, $y=\sim30$). The Ag-poor phase is present to a greater extent than the Ag-rich phase. The PSD phenomenon can be observed from this stage. (d) shows the phase-separated films with a higher Ag concentration than (c) ($x=\sim60$, $y=\sim35$). The Ag-rich phase is dominant with respect to the Ag-poor phase at this stage. (e) represents the films completely comprising the Ag-rich phase ($x=\sim67$, $y=\sim40$; maximum Ag content). The PSD phenomenon is the most pronounced at this stage. (f) depicts the films prepared with a higher deposition rate for Ag than (e). Metallic Ag particles are formed on the film surface during preparation, as indicated by the large dots.

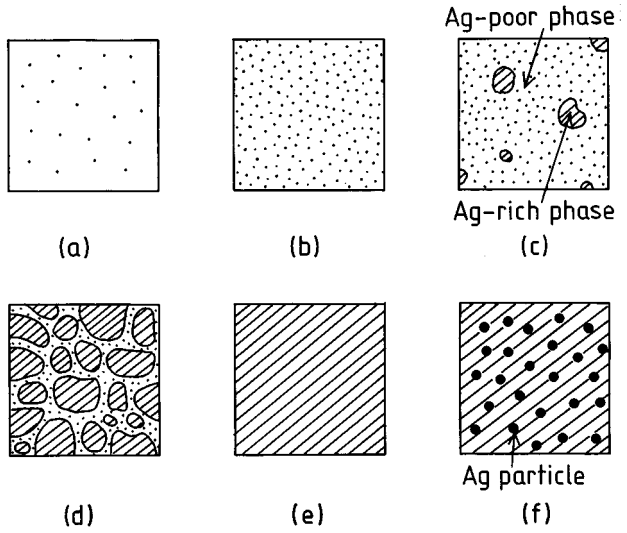

FIG. 13. Schematic illustration of the change in structure of S- and Se-based films with an increase in Ag content. The Ag content increases from (a) to (f). The small dots in (a)–(d) display schematically the Ag concentration, i.e., a high density means a high Ag concentration. The Ag concentration of the Ag-rich phase (hatched area) is close to the maximum Ag concentration. The large dots in (f) represent fine Ag particles formed on the film during preparation.

The PSD phenomenon was also observed for the annealed films and the photosensitivity was almost the same before and after annealing. Furthermore, it was found by SEM observation that most of the photodeposited Ag particles were located on the Ag-rich phase, suggesting that the PSD phenomenon appears only on the Ag-rich phase. This result agrees with the fact that the films with $x=\sim45$ and $y=\sim22$ did not exhibit the PSD phenomenon, since these films are considered to be comprised of the Ag-poor phase. The PSD phenomenon approximately increases in proportion to the increment of the Ag concentration beyond $x=45$ and $y=22$. This fact can be explained by the idea that the fraction of the Ag-rich phase increases corresponding to the increment of the Ag concentration.

All the phenomena observed for the S-based system were also observed for the Se-based system but the compositional ranges shifted to lower Ag concentration. This difference in the compositional ranges can be ascribed to the Ge–Se network structure being weaker than the Ge–S network structure against breaking up by Ag atoms through the formation of Ag–S(Se) ionic bonds, since Ge–Se bonds are weaker than Ge–S bonds.[23]

V. CONCLUSIONS

The optical, electrical, and structural properties of amorphous $(Ge_{0.3}S_{0.7})_{100-x}Ag_x$ and $(Ge_{0.3}Se_{0.7})_{100-y}Ag_y$ films have been studied over a wide composition range ($0\leqslant x\leqslant 67$, $0\leqslant y\leqslant 40$). The photoinduced and thermally induced phenomena of the Se-based system have also been examined and compared with existing data for the S-based system. The following conclusions can be reached from this study.

(i) The dc resistivity decreases drastically but the optical band gap decreases gradually with an increase in Ag content. These compositional trends resemble each other for both systems.

(ii) The Se-based films exhibit all the photoinduced and thermally induced phenomena observed for the S-based films. The compositional trends resemble each other but the phenomena for the Se-based system are observed at lower Ag concentration.

(iii) The structure of the S- and Se-based films depends significantly on the Ag content and the compositional trends resemble each other. Phase separation into Ag-poor and Ag-rich phases seems to occur in the Ag-rich films of both systems ($x>45$, $y>22$).

[1] T. Kawaguchi and S. Maruno, J. Appl. Phys. **77**, 628 (1995).
[2] A. V. Kolobov and S. R. Elliott, Adv. Phys. **40**, 625 (1991).
[3] S. Maruno, J. Non-Cryst. Solids **59–60**, 933 (1983).
[4] T. Kawaguchi and S. Maruno, Jpn. J. Appl. Phys. **33**, 6470 (1994).
[5] T. Kawaguchi, S. Maruno, and S. R. Elliott, J. Non-Cryst. Solids (in press).
[6] T. Kawaguchi, S. Maruno, and Ke. Tanaka, J. Appl. Phys. **73**, 4560 (1993).
[7] T. Kawaguchi, S. Maruno, and S. R. Elliott, J. Non-Cryst. Solids (in press).
[8] Y. Kawamoto and S. Tsuchihashi, J. Am. Ceram. Soc. **54**, 131 (1971).
[9] Z. V. Borisova, T. S. Rykova, E. Yu. Turkina, and A. R. Tabolin, Izv. Akad. Nauk SSSR, Neorg. Mater. **20**, 1796 (1984).
[10] L. Tichy, H. Ticha, K. Handlir, and K. Junek, Philos. Mag. Lett. **58**, 233 (1988).
[11] L. Tichy, V. Smrcka, H. Ticha, E. Sleecky, and P. Nagels, Philos. Mag. Lett. **68**, 73 (1993).
[12] L. Tichy, A. Triska, H. Ticha, and M. Frumar, Philos. Mag. B **54**, 219 (1986).
[13] M. L. Theye, A. Gheorghiu, C. Senemaud, M. F. Kotkata, and K. K. Kandil, Philos. Mag. B **69**, 209 (1994).
[14] P. Nagels, L. Tichy, A. Triska, and H. Ticha, J. Non-Cryst. Solids **77–78**, 1265 (1985).
[15] K. L. Bhatia, G. Parthasarathy, D. P. Gosain, and E. S. R. Gopal, Philos. Mag. B **51**, L63 (1985).
[16] P. S. L. Narasimham, A. Giridhar, and S. Mahadevan, J. Non-Cryst. Solids **43**, 365 (1981).
[17] Y. Kawamoto and M. Nishida, J. Non-Cryst. Solids **20**, 393 (1976).
[18] Y. Miyamoto, M. Itoh, and Ke. Tanaka, Solid State Commun. **92**, 895 (1994).
[19] A. Doi, H. Sakai, M. Yamamoto, T. Kawaguchi, and S. Maruno, Jpn. J. Appl. Phys. **29**, 313 (1990).
[20] R. J. Dejus, S. Susman, K. J. Volin, D. G. Montague, and D. L. Price, J. Non-Cryst. Solids **143**, 162 (1992).
[21] J. H. Lee, A. P. Owens, A. Pradel, A. C. Hannon, M. Ribes, and S. R. Elliott (unpublished).
[22] S. R. Elliott, J. Phys. Condens. Matter **4**, 7661 (1992).
[23] L. Pauling, *Nature of the chemical bond* (Cornell University Press, Ithaca, New York, 1960).